A method to estimate effective population size from linkage disequilibrium when generations overlap

Luis Alberto García Cortés[1], Frédéric Austerlitz[2], and M. Ángeles R. de Cara[2,3,4]

[1]Departamento de Mejora Genética Animal (INIA, CSIC) Ctra. de La Coruña, km 7,5, 28040 Madrid, Spain

[2]UMR 7206 EcoAnthropologie, CNRS/MNHN/Université Paris Diderot, Musée de l'Homme, Paris, France

[3]Centro de Investigação em Biodiversidade e Recursos Genéticos (CIBIO-UP), InBIO, Universidade do Porto, Porto, Portugal

[4]Corresponding author. angeles.decara@cibio.up.pt

Abstract

Effective population size (N_e) is a key parameter in evolutionary and conservation studies. It represents the number of individuals of an ideal panmictic population that would have the same genetic drift as the observed population and can be used to establish management programmes. Several methods have been developed to estimate this parameter. Currently, for studies with one sample in time, the simplest methods are based on linkage disequilibrium. These methods rely on simple models, and biases have been shown when populations deviate from the assumptions made in those models. This occurs in particular when populations are age-structured or have overlapping generations. Recently, several methods have been developed to correct such biases. Here, we develop analytical equations to predict linkage disequilibrium within age groups, and

use such results to infer cohort size from samples of newborn individuals. We can in turn use these equations to estimate N_e accurately for a variety of species. Furthermore, using publicly available data, we apply our method to the white-crowned sparrow (*Zonotrichia leucophrys*).

Introduction Linkage disequilibrium is the association between alleles at different loci within or between chromosomes. It depends on allelic frequencies, recombination, mutation and effective population size (N_e, Hill & Robertson 1968). Thus, it can be used to make inferences about effective size, a crucial parameter in evolutionary and conservation studies. It is commonly considered that populations with N_e smaller than 50 are endangered in the short-term and that conservation programmes are often necessary for such populations (Franklin 1980). Most analytical predictions on linkage disequilibrium (LD) have been obtained in populations with non-overlapping generations, and such simple models have allowed a whole body of research aiming at estimating N_e from LD, starting with the pioneering work of Sved (1971).

Sved followed the work of Hill & Robertson (1968), which showed how alleles at different positions in the genome tend to become associated in finite populations. He studied LD between two biallelic loci and established that it is equivalent to studying identity by descent (IBD). By analysing the temporal dynamics of the allelic frequencies at the two loci ignoring mutation, he derived an analytical formula establishing the relationship between N_e and LD. In later work, Sved & Feldman (1973) observed that IBD and inbreeding can be calculated either using correlations between frequencies or using probability methods. This led them to take into account sampling with replacement, which resulted in a slight modification of Sved's (1971) formula. Weir & Hill (1980) and Hill (1981) also developed methods to infer N_e from LD measures, taking into account sample sizes and mating systems.

This body of work was not much used for a long time on real data, with a few exceptions in *Drosophila* and human data (Loukas *et al* 1979; Malpica & Briscoe 1982; Piazza *et al* 1985). With the advent of dense genotyping data, in particular in humans and livestock, and the work of Hayes *et al* (2003) who developed methods for inferring current and ancestral N_e, such estimates have become common to the point where they constitute the prevailing method nowadays. In parallel to

theoretical works on the relationship between N_e and LD, there has been a growing body of research showing the effects of population and age structure on estimates of N_e. This started with the work of Felsenstein (1971) who derived equations for N_e given a known age structure and Hill (1972) showed that N_e in such populations is equal to that of a population with non-overlapping generations with the same variance in lifetime family size. Orive (1993) used a coalescent approach to generalise to populations with overlapping generations and sexual or asexual reproduction. These works have mostly been used to calculate N_e in populations once their age structure has been determined, without making use of information on linkage disequilibrium. Only recently methods using both LD and data on age structure have been developed to improve estimates of N_e (Robinson & Moyer 2013; Waples *et al* 2014). These works have shown that using only LD to infer N_e in populations with overlapping generations can result in biased estimates, and Waples *et al* (2014) introduced heuristic modifications to correct such biases.

Here we develop analytical methods to account for age structure in the estimates of N_e from linkage disequilibrium. We start by deriving equations for linkage disequilibrium measured via r^2 (Hill & Robertson 1968) in a scenario consisting in a population with several cohorts of varying fertility and survival rates. We use the equivalence between r^2 and identity by descent to relate these genetic measures to N_e. By inverting the system of equations derived, we can then estimate the cohort size and the effective population size from genetic data. Furthermore, we take advantage of our previous research (Garcia-Cortes *et al* 2019), to show the importance of dealing appropiately with frequencies or probabilities, and how they lead to very different results. Finally, we apply our method to publicly available data from the white-crowned sparrow (*Zonotrichia leucophrys*, Lipshutz *et al* 2017).

Methods and material

Throughout the paper, we consider populations of N individuals who are diploid and, therefore, correspond to populations $2N$ gametes. Sved's (1971) method defines Q as the probability of identity by descent (IBD) of two gametes at locus B given that locus A is also IBD. This probability Q is also called the joint homozygosity and represents the probability of no crossing

over between loci A and B since the common ancestor. Sved (1971) showed that $E\left(r^2\right) = Q$, where $r^2 = D^2/\left(p_A p_a p_B p_b\right)$ is a measure of linkage disequilibrium between loci A and B, and derived the following probability of joint homozygosity in the next generation, Q', as

$$Q^{'} = \frac{1}{2N}(1-c)^2 + \left(1 - \frac{1}{2N}\right) Q\,(1-c)^2\,, \tag{1}$$

where c is the recombination fraction between loci A and B and N is the effective population size. This size is defined in Kimura & Crow (1963), as the size of an idealised population with the same inbreeding or random genetic drift as the population under consideration. The recombination fraction is obtained as $c = 0.5\left(1 - e^{-2d}\right)$ where d is the map distance (Haldane 1919). This equation was later revised by Sved & Feldman (1973) as

$$L^{'} = \frac{1}{2N} + \left(1 - \frac{1}{2N}\right) L\,(1-c)^2\,. \tag{2}$$

where L is the probability of identity by descent between loci A and B, also called linked identity by descent (Sved 2019). In the original paper where this modification was added (Sved & Feldman 1973), the rationale was that the probability of IBD for two loci follows the same logic as the probability of IBD for one locus ($F_t = \frac{1}{2N} + (1 - \frac{1}{2N})F_{t-1}$). Sved (1971) had derived eq. 1 thinking of frequencies rather than probabilities.

Thus, while Q and L are similar in concept, one of them is not appropiate (Sved 2019). Q is the probability of joint IBD without replacement, while L is the probability of joint IBD, but allowing for replacement. Earlier work has shown that L, as derived in Sved & Feldman (1973), provides better estimations of $E\left[r^2\right]$ (Garcia-Cortes *et al* 2019).

Equations (1) and (2) were developed for populations with non-overlapping generations. Nevertheless, many species have overlapping generations and this cannot be ignored when evaluating the intensity of genetic drift (Felsenstein 1971), or calculating the equilibrium between genetic drift and recombination. Most importantly, researchers have used estimates of N_e based on these equations without much caution about potential pitfalls (Robinson & Moyer 2013; Waples

et al 2014).

In populations with age structure, following the notation of Felsenstein (1971), the new cohort of N_0 newborns is the progeny of some parental age groups. Every newborn has a probability p_i of coming from a parent of age i, such that $\sum_i p_i = 1$. Note that our N_0 is equivalent to Felsenstein's (1971) N_1, the number of individuals born every time unit. Thus, N_0 is not an effective size, but a census size. The probability of a newborn to live to age i is given by s_i (l_i in Felsenstein, 1971), so that the number of individuals that survive to age i is given by $N_i = s_i N_0$.

For convenience, we firstly derive the equations for **Q** when generations overlap. We then calculate the equivalent **L** from which we derive equations to calculate the number of newborns N_0. This, in turn, can be used to calculate N_e, the effective population size per generation. We then describe how simulations were performed. Lastly, we analyse an available dataset of white crowned sparrows (*Zonotrichia leucophrys*).

Analytical derivations for probabilities of joint IBD The full derivation for the evolution of **Q** and **L** is given in Appendix A and Appendix B, respectively. For each of them, a full system of equations is derived, which includes the probabilities of joint IBD (without replacement for **Q** and with replacement for **L**). Such system initially includes probabilities of joint IBD across all cohorts. For instance, in the case of **Q**, it includes all Q_{ij}'s, the probabilities of joint IBD between gametes of cohort i and cohort j. The system for **Q** reduces to

$$\begin{bmatrix} \frac{1}{(1-c)^2} - \sum_i p_i^2(1-\frac{1}{2N_i}) & -\alpha_1 & -\alpha_2 & \dots \\ -p_1(1-\frac{1}{2N_1}) & \frac{1}{(1-c)} - \beta_{11} & -\beta_{12} & \dots \\ -p_2(1-\frac{1}{2N_2}) & -\beta_{21} & \frac{1}{(1-c)} - \beta_{22} & \dots \\ \dots & \dots & \dots & \dots \end{bmatrix} \begin{bmatrix} Q^{eq}_{(00)} \\ Q^{eq}_{(01)} \\ Q^{eq}_{(02)} \\ \dots \end{bmatrix} = \begin{bmatrix} \sum_i \frac{p_i^2}{2N_i} \\ \frac{p_1}{2N_1} \\ \frac{p_2}{2N_2} \\ \dots \end{bmatrix}, \tag{3}$$

where $\beta_{ik} = \sum_j \delta_{|i-j|,k} p_j$ and $\alpha_k = \sum_i \sum_j \delta_{|i-j|,k} p_i p_j$. The function $\delta_{i,j}$ is Kroenecker's delta, that is, $\delta_{i,i} = 1$ and $\delta_{i,j} = 0$ for $i \neq j$.

Similarly, as shown in detail in Appendix B, at equilibrium, **L** follows

$$\begin{bmatrix} 1-\zeta_{11} & -\zeta_{12} & -\zeta_{13} & \dots & 0 & -\tau_1 & 0 & 0 & \dots \\ -\zeta_{21} & 1-\zeta_{22} & -\zeta_{23} & \cdots & 0 & 0 & -\tau_2 & 0 & \cdots \\ -\zeta_{31} & -\zeta_{32} & 1-\zeta_{33} & \cdots & 0 & 0 & 0 & -\tau_3 & \cdots \\ \vdots & \vdots & \vdots & \ddots & \vdots & \vdots & \vdots & \vdots & \\ -\varphi_1 & -\varphi_2 & -\varphi_3 & \cdots & 1 & -\gamma_1 & -\gamma_2 & -\gamma_3 & \cdots \\ 0 & 0 & 0 & \cdots & -\xi_1 & 1 & 0 & 0 & \cdots \\ 0 & 0 & 0 & \cdots & 0 & -\xi_2 & 1 & 0 & \cdots \\ 0 & 0 & 0 & \cdots & 0 & 0 & -\xi_3 & 1 & \cdots \\ \vdots & \vdots & \vdots & & \vdots & \vdots & \vdots & \vdots & \ddots \end{bmatrix} \begin{bmatrix} L_{01}^{eq} \\ L_{02}^{eq} \\ L_{03}^{eq} \\ \vdots \\ L_{00}^{eq} \\ L_{11}^{eq} \\ L_{22}^{eq} \\ L_{33}^{eq} \\ \vdots \end{bmatrix} = \begin{bmatrix} 0 \\ 0 \\ 0 \\ \vdots \\ \frac{1}{2N_0} \\ \varrho_1 \\ \varrho_2 \\ \varrho_3 \\ \vdots \end{bmatrix}, \tag{4}$$

where $\zeta_{ik} = (1-c)\beta_{ik}$, $\tau_i = (1-c)p_i$, $\varphi_k = \left(1 - \frac{1}{2N_0}\right)(1-c)^2\,\alpha_k$, $\gamma_k = \left(1 - \frac{1}{2N_0}\right)(1-c)^2\,p_k^2$, $\xi_i = \frac{1-\frac{1}{2N_i}}{1-\frac{1}{2N_{i-1}}}$ and $\varrho_i = \frac{1}{2N_i} - \frac{\xi_i}{2N_{i-1}}$.

Estimation of N_0 from linkage disequilibrium

As $E\left(r^2\right) = L$ (Sved & Feldman 1973), we can use the equations described in the previous section to estimate N_0 from observed values of linkage disequilibrium. We thus use eq. 15, eq. 16, eq. 17 and eq. 18, but considering N_0 as unknown and L_{00}^{eq} as observed for a given value of recombination frequency.

The equations for N_0 are nonlinear but can be solved by iterating

$$2N_0 = \frac{1 + (1-c)^2 \sum_k (\alpha_k L_{0k}^{eq} - p_k^2 L_{kk}^{eq})}{L_{00}^{eq} + (1-c)^2 \sum_k (\alpha_k L_{0k}^{eq} - p_k^2 L_{kk}^{eq})}, \tag{5}$$

and the rest of identities in eq. (4), that is

$$L_{0i}^{eq} = \frac{\sum_{j \neq i} \zeta_{ij} L_{0j}^{eq} + \tau_i L_{ii}^{eq}}{1 - \zeta_{ii}}, \tag{6}$$

and

$$L_{ii}^{eq} = \varrho_i + \xi_i L_{i-1,i-1}^{eq}. \tag{7}$$

Numerical analyses

We compared our analytical results with simulated results. For this purpose, we followed these steps in our simulations:

1. We drew the number of newborn gametes coming from each group age (n_i) using multinomial deviates $n_1, n_2, ... \sim M(N_0, p_1, p_2, ...)$, where p_i is the proportion of the $2N_0$ newborn gametes born from individuals from cohort i.

2. For each cohort i then

   (a) We drew the number of recombined ($nrec_i$) or non-recombined ($norec_i$) gametes from a binomial deviate $nrec_i \sim B(n_i, c)$.

   (b) We drew the number of non-recombined progeny carrying each haplotype (AB,ab,aB and Ab) following a multinomial distribution $M(norec_i, p_{AB}(i), p_{Ab}(i), p_{aB}(i), p_{ab}(i))$, where $p_{AB}(i)$,$p_{Ab}(i)$,$p_{aB}(i)$ and $p_{ab}(i)$ represent the haplotypic frequencies of cohort i.

   (c) We drew the number of recombined progeny carrying each haplotype from a multinomial distribution $M(rec_i, p_A(i)P_B, p_A(i)P_b, p_a(i)P_B, p_a(i)P_b)$, where $p_A(i)$ and $p_a(i)$ are the allelic frequencies of cohort i. P_B and P_b represent the allelic frequencies of the whole population.

3. We calculated the haplotypic frequencies of newborn individuals by adding up gametes from steps 2b and 2c.

4. For each cohort i

   (a) We then drew the number of individuals to be removed $died \sim B[N_{i-1}, (N_{i-1} - N_i)/N_{i-1}]$ using N_i and N_{i-1},

(b) The number of individuals carrying each haplotype to be removed was then drawn from $M\,(died, p_{AB}(i-1), p_{Ab}(i-1), p_{aB}(i-1), p_{ab}(i-1))$, where p are the haplotypic frequencies at group age $i-1$

(c) Individuals were eliminated to calculate the new haplotypic frequencies at each cohort i.

Recombined and non-recombined gametes at step 2a include gametes that have undergone an odd or even number of crossovers, respectively. These calculations were performed over 100,000 replicates, each of which with one pair of loci. Allelic frequencies were 1/2 at the beginning of each replicate.

Simulations with many markers over several chromosomes In order to take into account correlations between pairs of markers in the genome, and their effect on our estimates, we performed simulations for each scenario with either 1000 or 5000 markers distributed at random over 1, 5 or 10 chromosomes of 1M each. Allelic frequencies at the beginning of each replicate were drawn from a uniform distribution. For each newborn gamete, we drew two individuals from the existing cohorts, with probabilities following the contribution of each cohort (i.e., we drew a random number between 0 and 1, and if it falls between $\sum_{i=1}^{n} p_i$ and $\sum_{i=1}^{n+1} p_i$ then the contributing parent comes from cohort $n+1$). We generated recombinations within each of those individuals so that, on average, there was one recombination per chromosome. We repeated this process until N_0 newborns were generated. After 500 generations, we calculated r^2 for each segregating pair and using eqs.5, 6 and 7 we obtained an estimate of N_0 for each pair. We then calculated the harmonic mean of N_0 for each replicate.

Application to real data The programs required to infer N_0 and N_e from observed r^2 are available at `https://github.com/angelesdecara/OverlapNeLD`. We applied our method to available data from white-crowned sparrow (*Zonotrichia leucophrys nuttalli*) (Lipshutz *et al* 2017, 2016), whose age structure has been described in earlier works (Baker *et al* 1981; Waples & Yokota 2007). White crowned sparrows have approximately 5 fertile cohorts together with the newborns

(i.e. 6 cohorts). Fertile individuals leave between 2.5 and 3.3 offspring per unit time, and the survival probability from newborns to one unit time old is 0.18, and then every unit time this probability is reduced by half roughly. These life-history values have been scaled such that population size remains constant. Data from 169 individuals are available for 6419 SNPs obtained using genotyping-by-sequencing (GBS). They can be classified in three different groups, depending on whether they are ssp. nuttalli, ssp. pugetensis or admixed. We calculated N_0 and N_e using the values for the fraction of a cohort that survives to a certain age, and the mean number of offspring produced per generation by individuals of each age group from Waples & Yokota (2007), separately for each subspecies.

Linkage disequilibrium was estimated using the option `-geno-r2` of vcftools (Danecek *et al* 2011). Note that this measure of linkage disequilibrium is the correlation between allelic frequencies not taking into account gametic phases. Thus, it is an approximation of the gametic linkage disequilibrium. Furthermore, there is no chromosome scale reference genome for this species, and the number of data was small. We corrected this estimate of r^2 to account for sample size following Weir & Hill (1980); Waples (2006); Waples & Do (2008), by the harmonic sample size for each pair of loci (see Waples & Do 2008, for further details).

As there is no available linkage map, we had no information on the positions of each SNP. Thus, we assumed that $c = 0.5$, that is, that all SNPs were independent. Thus, the results here obtained are likely to be downward biased. In order to infer the effective population size from N_0, we followed the approach developed by Felsenstein (1971), which we solved with using a recursive formula. We compared our results with those obtained using `Ne estimator` (Waples & Do 2008) based on LD using all informative SNPs, equally assuming that SNPs are unlinked.

In order to provide a standard error, we performed a jackknife approach (Waples *et al* 2020; Jones *et al* 2016). Considering a sample size of n individuals, we selected $n - 1$ individuals n times. For each jackknife sample we calculated R^2 (Waples & Do 2008), that is, the weighted correlation between genotype frequencies at different markers, corrected by sample size. Realistic sample sizes generate linkage disequilibrium due to sampling, and this needs to be corrected before

applying any method to estimate N_e (Waples 2006; Waples & Do 2008). Once we have R^2 for each jackknife sample, we obtained N_0 and from there N_e, which allowed us to obtain a standard error for both values. Similarly, we could have obtained the bounds of the confidence interval for R^2 and use our equations to obtain the bounds for N_e. Furthermore, we tested the effect of considering all loci, independently of their minor allele frequency (MAF), or only those with MAF greater than 0.05.

Results

We compare here the results obtained analytically with those obtained computationally using multinomial distributions, following the above algorithm. The population here studied consists of three fertile cohorts or age groups, that produce N_0 newborns. We studied the three following scenarios:

1. All contributions are the same (i.e. all N_i's take the same value of 1000 individuals) and $p_1 = p_2 = p_3 = \frac{1}{3}$.

2. All cohorts have the same number of individuals (all $N_i = 1000$ individuals), but they contribute differently to the number of newborns, due to different fertilities per age group, such that $p_1 = 0.3$, $p_2 = 0.5$ and $p_3 = 0.2$.

3. Cohorts have different sizes ($N_1 = 1000$, $N_2 = 800$ and $N_3 = 500$) and contribute differently $p_1 = 0.3$, $p_2 = 0.5$ and $p_3 = 0.2$.

Fig. 3 shows analytical and simulated results for L_{00}, in black and green respectively, for a population with 3 cohorts and $N_0 = 1000$ individuals. The difference between the estimated (L_{00} as given by eqs. 15, 16 and 17) and the average r^2 using 100,000 replicates (that is, estimated from L_{00} is larger as the contribution of one cohort increases as compared to the other cohorts, and furthermore, this difference increases with cohort age. In other words, the difference between estimated and observed when cohort 1 is the only one contributing is zero, but when cohort 3 is the most contributing this difference is larger than when cohort 2 is the most contributing.

As shown in tab. 1, we can see how linkage disequilibrium as measured by r^2 is in very good agreement with the results obtained for L_{00} (eqs. 15, 16 and 17), which takes into account sampling with replacement, while Q_{00} (eq. 3) differs noticeably. This is the case for the three scenarios, with the difference between r^2 and Q_{00} increasing with increasing complexity. Scenario 3 shows the largest differences between r^2 and L_{00}, but both measures are still in very good agreement, for a variety of recombination probabilities.

Estimates of N_0 from L_{00} are shown in tab. 2, where we used the 100,000 results to provide the average, and then we used sets of either 100 or 500 pairs of loci to provide the standard deviation In both cases, the results are for $N_0 = 1000$ individuals and we can see how the inferred N_0 is mostly accurate within 15% deviation when 100 replicates are used and within 7% when 500 replicates are used.

Lastly, we have analysed the dependence on c and N_0 (eq. 5). In fig. 4, we can see how the inferred N_0 deviates from its true value of 1000 depending on the recombination fraction c. This deviation is stronger for tighter linkage, i.e. small c. In fig. 5, we can see how the inferred N_0 has a high accuracy under all scenarios for all recombination rates.

A detailed analysis of the estimated N_0 versus recombination frequency is shown in Fig. 4, where we can see the three scenarios studied. Overall, the larger the recombination frequency, the better the estimate of N_0.

Similar results are shown in Fig. 5, where we can see the dependency of the estimated N with its true value for four recombination frequencies. The estimate provides a good result overall.

Results on simulations with 1000 or 5000 markers randomly allocated in either 1, 5 or 10 chromosomes are shown in Table 3. The estimates are consistently good, and standard deviation decreases with number of chromosomes, as most measurements of r^2 is between markers in different chromosomes, which results in the most accurate estimates of N_0.

Application to real data: white crowned sparrows Using the life-history parameters from Waples & Yokota (2007) and our exact equations, we inferred N_0, and then, using the recursive equations from Felsenstein (1971), we used this result to infer N_e. Results on inferred N_e are shown in

Table 4. There we can see that the inferred N_e is rather low, which would indicate the need for a conservation programme. It is however possible that this low N_e is partly due to the assumption of independent SNPs, and using a different value of c would result in larger estimates of N_e.

The estimates for N_e are considerably lower than those obtained by Lipshutz *et al* (2017) using fastsimcoal (Excoffier *et al* 2013), which uses the site frequency spectrum (SFS) to make demographic inferences. This discrepancy between estimates based on LD or those based on fastsimcoal using the SFS has been observed in other studies (Sovic *et al* 2019). The differences may be due to several factors, like the fact that Lipshutz *et al* (2017) assumed constant population sizes throughout long time-scales, and allowed for migration (Santiago *et al* 2020).

Discussion

Following Sved (1971); Sved & Feldman (1973) and earlier work (Garcia-Cortes *et al* 2019), we have derived here exact equations for linkage disequilibrium in populations with overlapping generations. Combining this result with life-history parameters, we have inferred the number of newborns per generation, N_0, which in turn, can be used to estimate effective population size, a key parameter in evolutionary and conservation studies. We have derived estimates per generation, not per year, and thus, we have not derived N_b, the effective population size per year. The strength of our method is that we do not require any approximation, as it relies on an analytical approach.

Our goal here was partly to take into account the developments made by Sved & Feldman (1973); Sved (2019) so that sampling with replacement is considered. Sved (2019) emphasised the linked identity by descent (L), which is conceptually equivalent to what he called earlier (Sved 1971) joint identity by descent (Q). Both identities are related by equations (13) and (14). Our goal was to develop a model-based method, and thus we have not compared our results with the heuristic approach of Waples *et al* (2014).

Our results show that using the linked identity by descent provides better estimates, which is in agreement with our earlier work (Garcia-Cortes *et al* 2019). We have further compared our exact results with those obtained via simulations, using multinomial distributions, and have obtained a very good agreement between them.

Our method is reliable and behaves well even with a strong age-structure, as seen on Fig. 4 and Fig. 5. Based on Fig. 4, the best estimates are obtained for loosely linked or unlinked markers. The good agreement can also be observed in Fig. 3, where we can see the good agreement between the estimated and the simulated size. It seems that the older the most contributing cohort, the largest the differences between the estimated and the simulated size. Even so, the estimates are very good and mostly within 10% relative error.

We have developed equations to infer N_e starting from L_{00}, that is, linkage disequilibrium within newborns. Using such measure, we can derive all linkage disequilibria within and between cohorts, which leads to the inference of N_e by using the sets of equations(4). Alternatively, we could take a random sample from the population to estimate overall linkage disequilibrium. In that case, we could infer N_e combining this overall estimate of LD, which is the weighted sum of the linkage disequilibria between and within cohorts. This would add further complexity to the problem, as it would require equations(4) together with this weighted average.

Our method is based on a set of assumptions, and therefore, it has to be applied with caution. In order to derive analytical results, we have assumed constant population and cohort sizes, as well as constant life-history parameters. We have assumed random mating, and thus, variance in mean reproductive success is equal to the mean.

Finally, we have used our analytical results to infer N_e in the white-crowned sparrow, for which genetic and demographic data were available (Baker *et al* 1981; Lipshutz *et al* 2017). The results shown in Tab. 4 are in line with our previous results. We had shown for non-overlapping generations that the estimator of Weir & Hill (1980) was downward biased (Garcia-Cortes *et al* 2019). In Table 4 we observe a similar trend, where the results obtained with `Ne estimator`, based on the estimator developed by Weir & Hill (1980), are smaller than those obtained with our method. We have to emphasise that this dataset suffers from a small sample size, lack of linkage map and using an estimate of r^2, as gametic phases are unavailable. Furthermore, we have used life-history parameters that were estimated in one population of the subspecies. Our results are limited by the information we have, and thus should be taken with caution.

Obiously, our results are still limited by the assumptions here made, like constant age structure and constant population size. We warn researchers working in species or populations who are aware of huge expansions or bottlenecks or fluctuating size that this is probably not the most appropiate method to analyse their data. Most importantly, life-history parameters need to be adjusted so that population size is constant (Waples & Yokota 2007). Our method does not work and will give incorrect results if this premise is not held. Some populations may have extremely succesful individuals who leave a large number of offspring. This is a well-known issue when estimating effective population size. We have assumed a Poisson distribution in the reproductive success, and thus, deviations from this distribution may bias the result.

Genomic data are now easily accessible, yet, there are two issues which may make our method not straightforward. The first one is lack of life-history parameters, which require long-term studies to characterise survival and fertility. The second one is the lack of reference genomes. Our method can be applied to any type of genomic data, and ideally a recombination map should be available. Otherwise, we recommend filtering the data by minor allele frequencies (Jones *et al* 2016, and references therein), as rare alleles are known to bias the inference, and assume free recombination for unmapped markers from RADseq or GBS. For those cases where scaffolds are available, keep one SNP from each scaffold, and depending on genome size and number of markers and scaffolds, analyse them as unlinked. Based on our simulations, we think that there where sequence data are available, we believe using about 10000 good quality evenly sparsed throughout the genome is more than enough.

This study shows the potential of our method to make estimates of effective population size in wild species using the available programs at `http://github.com/angelesdecara/OverlapNeLD`.

Acknowledgements This work was funded by Ministerio de Economía y Competitividad grant number AGL2016-75942-R, by the LabEx BCDIV (ANR-10-LABX-0003-BCDiv), within the framework of the program “Investing for the future” (ANR-11-IDEX-0004-02) and by the Agence Nationale de la Recherche project AGRHUM (ANR-14-CE02-0003). We are most grateful to Elizabeth Derryberry, Sara Lipshutz, Amy Luo and Ryan Waples for feedback on the data and the

manuscript. The cluster Finis Terrae II at Centro de Computación de Galicia was used for this work.

*

References

Baker M, Mewaldt LR, Stewart RM (1981) Demography of white-crowned sparrows (*zonotrichia leucophrys nuttalli*). *Ecology*, **62**, 636–644.

Danecek P, Auton A, Abecasis G, *et al* (2011) The variant call format and vcftools. *Bioinformatics*, **27**, 2156–2158.

Excoffier L, Dupanloup I, Huerta-Sánchez E, Sousa VC, Foll M (2013) Robust demographic inference from genomic and snp data. *PLOS Genetics*, **9**, 1–17.

Felsenstein J (1971) Inbreeding and variance effective numbers in populations with overlapping generations. *Genetics*, **68**, 581–597.

Franklin IR (1980) Evolutionary change in small populations. In *Conservation Biology: An Evolutionary Ecological Perspective* (edited by ME Soule, BA Wilcox), pp. 135–140. Sinauer Assocs, Sunderland, Mass.

Garcia-Cortes LA, Austerlitz F, de Cara MAR (2019) An evaluation of the methods to estimate effective population size from measures of linkage disequilibrium. *J Evol Biol*, **32**, 267–277.

Haldane J (1919) The combination of linkage values, and the calculation of distances between the lociof linked factors. *J Genetics*, **8**, 299–309.

Hayes BJ, Visscher PM, McPartlan HC, Goddard ME (2003) Novel multilocus measure of linkage disequilibrium to estimate past effective population size. *Genome Res.*, **13**, 635–643.

Hill W (1972) Effective size of populations with overlapping generations. *Theoretical Population Biology*, **3**, 278+.

Hill WG (1981) Estimation of effective population size from data on linkage disequilibrium. *Genet. Res.*, **38**, 209–216.

Hill WG, Robertson A (1968) Linkage disequilibrium in finite populations. *Theor and Appl Genet*, **38**, 226–231.

Jones AT, Ovenden JR, Wang YG (2016) Improved confidence intervals for the linkage disequilibrium method for estimating effective population size. *Heredity*, **117**, 217–223.

Kimura M, Crow JF (1963) The measurement of effective population number. *Evolution*, **17**, 279–288.

Lipshutz SE, Overcast IA, Hickerson MJ, Brumfield RT, Derryberry EP (2016) Data from: Behavioral response to song and genetic divergence in two subspecies of white-crowned sparrows (*zonotrichia leucophrys*), Dryad, Dataset. https://doi.org/10.5061/dryad.5jc0t.

Lipshutz SE, Overcast IA, Hickerson MJ, Brumfield RT, Derryberry EP (2017) Behavioural response to song and genetic divergence intwo subspecies of white-crowned sparrows (*zonotrichia leucophrys*). *Molecular Ecology*, **26**, 3011–3027.

Loukas M, Krimbas C, Vergini Y (1979) Genetics of drosophila-subobscura populations .9. studies on linkage disequilibrium in 4 natural-populations. *Genetics*, **93**, 497–523.

Malpica J, Briscoe D (1982) Multilocus nonrandom associations in drosophila-melanogaster. *GENETICS RESEARCH*, **39**, 41–61.

Orive M (1993) Effective population size in organims with complex life-histories. *Theor. Pop. Biol.*, **44**, 316–340.

Piazza A, Mayr WR, Contu L, *et al* (1985) Genetic and population structure of four sardinian villages. *Annals of Human Genetics*, **49**, 47–63.

Robinson JD, Moyer GR (2013) Linkage disequilibrium and effective population size when generations overlap. *Evol Apps*, **6**, 290–302.

Santiago E, Novo I, Pardiãs AF, Saura M, Wang J, Caballero A (2020) Recent Demographic History Inferred by High-Resolution Analysis of Linkage Disequilibrium. *Molecular Biology and Evolution*, **37**, 3642–3653.

Sovic M, Fries A, Martin S, Lisle Gibbs H (2019) Genetic signatures of small effective population sizes and demographic declines in an endangered rattlesnake, *sistrurus catenatus*. *Evolutionary Applications*, **12**, 664–678.

Sved JA (1971) Linkage disequilibrium and homozygosity of chromosome segments in finite populations. *Theor Pop Biol*, **2**, 125–141.

Sved JA (2019) Linkage disequilibrium (ld). http://www.handsongenetics.com/PIFFLE/LinkageDisequilibrium.pdf.

Sved JA, Feldman MW (1973) Correlation and probability methods for one and two loci. *Theor Pop Biol*, **4**, 129–132.

Waples RK, Waples RS, Ward EJ (2020) Pseudoreplication in genomics-scale datasets. *bioRxiv*.

Waples RS (2006) A bias correction for estimates of effective population size based on linkage disequilibrium at unlinked gene loci. *Conservation Genetics*, **7**, 167–184.

Waples RS, Antao T, Luikart G (2014) Effects of overlapping generations on linkage disequilibrium estimates of effective population size. *Genetics*, **197**, 769–780.

Waples RS, Do C (2008) LDNe: a program for estimating effective population size from data on linkage disequilibrium. *Mol Ecol Res*, **8**, 753–756.

Waples RS, Yokota M (2007) Temporal estimates of effective population size in species with overlapping generations. *Genetics*, **175**, 219–233.

Weir BS, Hill WG (1980) Effect of mating structure on variation in linkage disequilibrium. *Genetics*, **95**, 477–488.

Appendix A: Dynamics of Q throughout generations Following the notation for Q of Sved (1971), we denote Q_{ij} as the probability of joint homozygosity between a pair of gametes from age groups i and j and Q_{ii} is such probability between two different gametes of the same age group i, *i.e.* two gametes sampled without replacement. Then, at a given time interval,

$$\mathbf{Q} = \left[\begin{array}{c|cccc} Q_{00} & Q_{01} & Q_{02} & Q_{03} & \cdots \\ \hline Q_{10} & Q_{11} & Q_{12} & Q_{13} & \cdots \\ Q_{20} & Q_{21} & Q_{22} & Q_{23} & \cdots \\ Q_{30} & Q_{31} & Q_{32} & Q_{33} & \cdots \\ \vdots & \vdots & \vdots & \vdots & \ddots \end{array}\right]$$

where 0 is the group of newborns. The definition of matrix **Q** here mimics the definition of the heterozygosity matrix in Felsenstein (1971).

We denote Q'_{ij} as the elements of **Q** at the next time unit. Every time unit the Q at each cohort can be written in terms of contributions from other Qs at other cohorts, and analogously for between cohorts Q_{ij}. In fig. 1, we show the five possible origins of a pair of random gametes in a population with two parental age groups. This can be easily extended for $\left(n^2 + 3n\right)/2$ contributions with n parental groups. The recursive formula to obtain Q'_{00}, i.e. Q_{00} at the next time unit, given the elements of **Q** can be obtained adding all contributions on fig. 1. This can be generalised to any number of age groups such that

$$\begin{aligned} Q'_{00} &= (1-c)^2 \sum_i p_i^2 \left[\frac{1}{2N_i} + \left(1 - \frac{1}{2N_i}\right) Q_{ii}\right] \\ &+ 2\,(1-c)^2 \sum_i \sum_{j<i} p_i p_j Q_{ij}, \end{aligned} \tag{8}$$

where the term $(1-c)^2 \sum_i p_i^2 \left[\frac{1}{2N_i} + \left(1 - \frac{1}{2N_i}\right) Q_{ii}\right]$ corresponds to the sum of the contribution of cases (a), (b), (d) and (e) in fig. 1 while the term $2\,(1-c)^2 \sum_i \sum_{j<i} p_i p_j Q_{ij}$ corresponds to case (c) extended for an arbitrary number of cohorts. In order to derive the probabilities of each case, and following Sved (1971), the term $(1-c)^2$ accounts for no crossover in either maternal or paternal

meiosis, while p_i^2 or $p_i p_j$ is the probability of a pair of gametes to come from the same or different age groups. Lastly, $\frac{1}{2N_i}$ and $\left(1 - \frac{1}{2N_i}\right)$ denote the probabilities that ancestral gametes to be identical or not, respectively.

Fig. 2 shows the contributions of the three possible cases for both Q'_{01} and Q'_{02} (or $n + 1$ contributions for n age groups). Adding all contributions for an arbitrary number of age groups, the recursive formula to obtain each Q'_{0i} is

$$\begin{aligned} Q'_{0i} &= (1-c)\, p_i \left[\frac{1}{2N_i} + \left(1 - \frac{1}{2N_i}\right) Q_{ii} \right] \\ &+ (1-c) \sum_{j \neq i} p_j Q_{ij}. \end{aligned} \tag{9}$$

Given that individuals from cohort i will move onto cohort $i + 1$ in the next time unit, the joint homozygosity between survivors of cohort i and cohort j in a time unit remains the same in the next time unit. Therefore, the remaining elements in $\mathbf{Q}'$ are

$$Q'_{ij} = Q_{i-1,j-1}, \tag{10}$$

and

$$Q'_{ii} = Q_{i-1,i-1}. \tag{11}$$

The recursive formulae given by eq. (8) to eq. (11) reach an equilibrium $\mathbf{Q}^{eq}$ where drift and recombination balance out. At equilibrium $Q'_{ij} = Q_{ij}$ and, considering eq. (10) and eq. (11), it follows that $Q_{00} = Q_{11} = Q_{22}$, $Q_{01} = Q_{12} = Q_{23}$, $Q_{02} = Q_{13}$ and so on. Thus, the matrix given by

$$\mathbf{Q}^{eq} = \left[\begin{array}{c|cccc} Q^{eq}_{(00)} & Q^{eq}_{(01)} & Q^{eq}_{(02)} & Q^{eq}_{(03)} & \cdots \\ \hline Q^{eq}_{(01)} & Q^{eq}_{(00)} & Q^{eq}_{(01)} & Q^{eq}_{(02)} & \cdots \\ Q^{eq}_{(02)} & Q^{eq}_{(01)} & Q^{eq}_{(00)} & Q^{eq}_{(01)} & \cdots \\ Q^{eq}_{(03)} & Q^{eq}_{(02)} & Q^{eq}_{(01)} & Q^{eq}_{(00)} & \cdots \\ \vdots & \vdots & \vdots & \vdots & \ddots \end{array} \right]$$

and equations (8) and (9) can be solved using

$$\begin{bmatrix} \frac{1}{(1-c)^2} - \sum_i p_i^2(1-\frac{1}{2N_i}) & -\alpha_1 & -\alpha_2 & \dots \\ -p_1(1-\frac{1}{2N_1}) & \frac{1}{(1-c)} - \beta_{11} & -\beta_{12} & \dots \\ -p_2(1-\frac{1}{2N_2}) & -\beta_{21} & \frac{1}{(1-c)} - \beta_{22} & \dots \\ \dots & \dots & \dots & \dots \end{bmatrix} \begin{bmatrix} Q^{eq}_{(00)} \\ Q^{eq}_{(01)} \\ Q^{eq}_{(02)} \\ \dots \end{bmatrix} = \begin{bmatrix} \sum_i \frac{p_i^2}{2N_i} \\ \frac{p_1}{2N_1} \\ \frac{p_2}{2N_2} \\ \dots \end{bmatrix}, \tag{12}$$

where $\beta_{ik} = \sum_j \delta_{|i-j|,k} p_j$ and $\alpha_k = \sum_i \sum_j \delta_{|i-j|,k} p_i p_j$. The function $\delta_{i,j}$ is Kroenecker's delta, that is, $\delta_{i,i} = 1$ and $\delta_{i,j} = 0$ for $i \neq j$.

Appendix B: Dynamics of L throughout generations

Here, we derive the equations for L, the probability of linked identity by descent, at two positions, as defined by Sved & Feldman (1973) and Sved (2019). We define L_{ij} as the LIBD of a pair of gametes from age groups i and j and L_{ii} as the LIBD of two gametes of age group i, drawn at random with replacement. Then, at any given generation, L is given by

$$\mathbf{L} = \left[\begin{array}{c|cccc} L_{00} & L_{01} & L_{02} & L_{03} & \cdots \\ \hline L_{10} & L_{11} & L_{12} & L_{13} & \cdots \\ L_{20} & L_{21} & L_{22} & L_{23} & \cdots \\ L_{30} & L_{31} & L_{32} & L_{33} & \cdots \\ \vdots & \vdots & \vdots & \vdots & \ddots \end{array}\right].$$

Following the relationships derived in appendix **C**, the relationship between Q and L is thus:

$$L_{ij} = Q_{ij}, \text{for } i \neq j, \tag{13}$$

and

$$L_{ii} = \frac{1}{2N_i} + \left(1 - \frac{1}{2N_i}\right) Q_{ii}. \tag{14}$$

To calculate L'_{00}, we replace eq. (13) and eq. (14) in eq. (8):

$$\begin{aligned} Q'_{00} &= (1-c)^2 \sum_i p_i^2 L_{ii} + 2\,(1-c)^2 \sum_i \sum_{j<i} p_i p_j L_{ij} \\ &= (1-c)^2 \sum_i \sum_j p_i p_j L_{ij}, \end{aligned}$$

and replacing in eq. (14), we obtain that

$$L'_{00} = \frac{1}{2N_0} + \left(1 - \frac{1}{2N_0}\right)(1-c)^2 \sum_i \sum_j p_i p_j L_{ij}. \tag{15}$$

Similarly, to calculate L'_{0i}, we replace both eq. (13) and eq. (14) in eq. (9), obtaining

$$\begin{aligned} Q'_{0i} &= (1-c)\, p_i L_{ii} + (1-c) \sum_{j \neq i} p_j L_{ij} \\ &= (1-c) \sum_j p_j L_{ij}. \end{aligned}$$

We can use these results in eq. (13):

$$L'_{0i} = (1-c) \sum_j p_j L_{ij}. \tag{16}$$

It then follows from eq. (10) and eq. (13) that

$$L'_{ij} = L_{i-1,j-1}. \tag{17}$$

In fact, sampling with or without replacement are equivalent when considering gametes from different age groups. Finally, to calculate L'_{ii} we rewrite eq. (14) as

$$Q_{ii} = \frac{L_{ii} - \frac{1}{2N_i}}{1 - \frac{1}{2N_i}},$$

and replace it in eq. (11), which results in

$$L'_{ii} = \frac{1}{2N_i} + \frac{1 - \frac{1}{2N_i}}{1 - \frac{1}{2N_{i-1}}} \left(L_{i-1,i-1} - \frac{1}{2N_{i-1}}\right). \tag{18}$$

Using all the above results, eq. (18) can be rewritten as

$$L_{ii} = \frac{1}{2N_i} + \frac{1-\frac{1}{2N_i}}{1-\frac{1}{2N_0}}\left(L_{00} - \frac{1}{2N_0}\right). \tag{19}$$

At equilibrium, $L'_{ij} = L_{ij}$ and, following eq. (17), $L_{01} = L_{12} = L_{23}$, $L_{02} = L_{13}$, ... and so on. Thus,

$$\mathbf{L}_{eq} = \left[\begin{array}{c|cccc} L^{eq}_{00} & L^{eq}_{01} & L^{eq}_{02} & L^{eq}_{03} & \cdots \\ \hline L^{eq}_{01} & L^{eq}_{11} & L^{eq}_{01} & L^{eq}_{02} & \cdots \\ L^{eq}_{02} & L^{eq}_{01} & L^{eq}_{22} & L^{eq}_{01} & \cdots \\ L^{eq}_{03} & L^{eq}_{02} & L^{eq}_{01} & L^{eq}_{33} & \cdots \\ \vdots & \vdots & \vdots & \vdots & \ddots \end{array}\right]. \tag{20}$$

Therefore, at equilibrium

$$\begin{bmatrix} 1-\zeta_{11} & -\zeta_{12} & -\zeta_{13} & \dots & 0 & -\tau_1 & 0 & 0 & \dots \\ -\zeta_{21} & 1-\zeta_{22} & -\zeta_{23} & \cdots & 0 & 0 & -\tau_2 & 0 & \cdots \\ -\zeta_{31} & -\zeta_{32} & 1-\zeta_{33} & \cdots & 0 & 0 & 0 & -\tau_3 & \cdots \\ \vdots & \vdots & \vdots & \ddots & \vdots & \vdots & \vdots & \vdots & \\ -\varphi_1 & -\varphi_2 & -\varphi_3 & \cdots & 1 & -\gamma_1 & -\gamma_2 & -\gamma_3 & \cdots \\ 0 & 0 & 0 & \cdots & -\xi_1 & 1 & 0 & 0 & \cdots \\ 0 & 0 & 0 & \cdots & 0 & -\xi_2 & 1 & 0 & \cdots \\ 0 & 0 & 0 & \cdots & 0 & 0 & -\xi_3 & 1 & \cdots \\ \vdots & \vdots & \vdots & & \vdots & \vdots & \vdots & \vdots & \ddots \end{bmatrix} \begin{bmatrix} L^{eq}_{01} \\ L^{eq}_{02} \\ L^{eq}_{03} \\ \vdots \\ L^{eq}_{00} \\ L^{eq}_{11} \\ L^{eq}_{22} \\ L^{eq}_{33} \\ \vdots \end{bmatrix} = \begin{bmatrix} 0 \\ 0 \\ 0 \\ \vdots \\ \frac{1}{2N_0} \\ \varrho_1 \\ \varrho_2 \\ \varrho_3 \\ \vdots \end{bmatrix}, \tag{21}$$

where $\zeta_{ik} = (1-c)\beta_{ik}$, $\tau_i = (1-c)p_i$, $\varphi_k = \left(1-\frac{1}{2N_0}\right)(1-c)^2\,\alpha_k$, $\gamma_k = \left(1-\frac{1}{2N_0}\right)(1-c)^2\,p_k^2$, $\xi_i = \frac{1-\frac{1}{2N_i}}{1-\frac{1}{2N_{i-1}}}$ and $\varrho_i = \frac{1}{2N_i} - \frac{\xi_i}{2N_{i-1}}$.

It is well known that sampling with replacement usually leads to equations simpler than those derived considering sampling without replacement. For this reason, eq. (15) and eq. (16) are simpler than eq. (8) and eq. (9). Nevertheless, the number of equations to solve for L^{eq} is larger

than the number of equations required to solve Q^{eq}, which accounts for differences between the diagonal elements of matrix (20).

Appendix C: Note on relation between Sved (1971) and Sved & Feldman (1973)

Both methods are equivalent, but the first develops equations for Q while the latter iterates L. As it seems $L = r^2$, both methods are equivalent if

$$L = \frac{1}{2N} + \left(1 - \frac{1}{2N}\right) Q. \tag{22}$$

Sved (1971) develops the following recursive equation

$$Q^{'} = (1-c)^2 \frac{1}{2N} + (1-c)^2 \left(1 - \frac{1}{2N}\right) Q, \tag{23}$$

while Sved & Feldman (1973) develop recursive equations for

$$L^{'} = \frac{1}{2N} + (1-c)^2 \left(1 - \frac{1}{2N}\right) L. \tag{24}$$

We can show this by replacing L and $L^{'}$ in eq. (24) using eq. (22):

$$\frac{1}{2N} + \left(1 - \frac{1}{2N}\right) Q^{'} = \frac{1}{2N} + (1-c)^2 \left(1 - \frac{1}{2N}\right) \left[\frac{1}{2N} + \left(1 - \frac{1}{2N}\right) Q\right]$$

and, replacing $Q^{'}$, it coincides with eq. (23):

$$Q^{'} = (1-c)^2 \left[\frac{1}{2N} + \left(1 - \frac{1}{2N}\right) Q\right].$$

Figure 1: Inheritance of gametes in a scenario with two cohorts. Left: (A) Probability of two gametes (on gray) to be offspring of the same gamete one cohort back in time. (B) Probability of two gametes to be offspring from two independent gametes one cohort back in time Case (C) shows two gametes that are offspring from gametes from two different cohorts. In case (D) two gametes are offspring from the same gamete two cohorts back in time. Lastly, in case (E), two gametes who descend from two different gametes two cohorts back in time. On the right, the probabilities of each case (A)-(E).

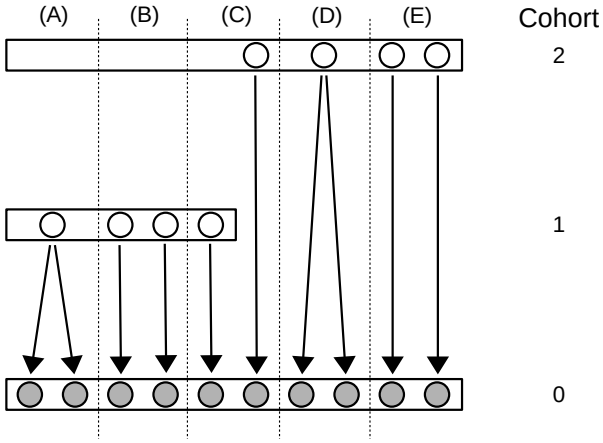

(A) $(1-c)^2\, p_1^2 \frac{1}{2N_1}$

(B) $(1-c)^2\, p_1^2 \left(1 - \frac{1}{2N_1}\right) Q_{11}$

(C) $(1-c)^2\, 2p_1 p_2 Q_{12}$

(D) $(1-c)^2\, p_2^2 \frac{1}{2N_2}$

(E) $(1-c)^2\, p_2^2 \left(1 - \frac{1}{2N_2}\right) Q_{22}$

Figure 2: Probability of two gray gametes to be IBD given that one is offspring from the white gamete. Cases A to C show all conditional IBD between two gametes of successive cohorts, while cases D to F illustrate conditional IBD between two gametes born two cohorts apart. Probabilities are shown on the right.

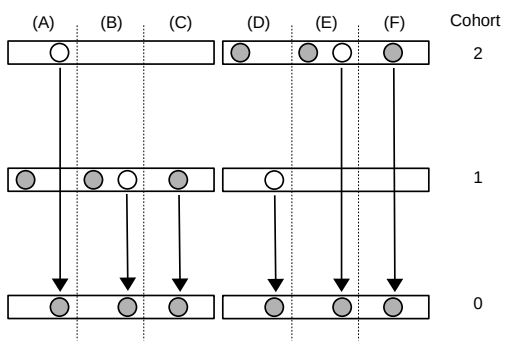

(A)	$(1-c)\,p_2 Q_{12}$
(B)	$(1-c)\,p_1\left(1-\frac{1}{2N_1}\right)Q_{11}$
(C)	$(1-c)\,p_1\frac{1}{2N_1}$
(D)	$(1-c)\,p_1 Q_{12}$
(E)	$(1-c)\,p_2\left(1-\frac{1}{2N_2}\right)Q_{22}$
(F)	$(1-c)\,p_2\frac{1}{2N_2}$

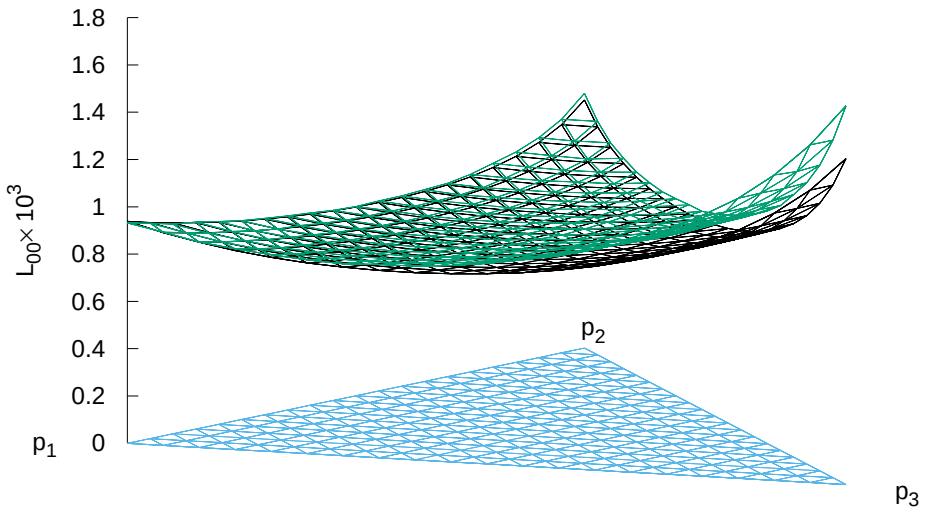

Figure 3: Equilibrium values for L_{00} obtained via analytical results (black), simulations using multinomial distributions (green). $N_0 = 1000$ individuals and loci are assumed to be at 50cM. The triangle axis represent the contribution from each cohort p_i to the pool of newborns, which satisfy $\sum_{i=1}^{3} p_i = 1$.

Table 1: Results for r^2 evaluated for three scenarios, for different genetic distances (d) which correspond to different recombination rates (c). Results are given evaluated using multinomial distributions ("Empirical r^2"), from Q_{00} or measured from L_{00}. Scenario 1: All contributions are the same (i.e. all N_i's take the same value equal to 1000 individuals) and $p_1 = p_2 = p_3 = \frac{1}{3}$. Scenario 2: All contributions are the same (all $N_i = 1000$ individuals), but $p_1 = 0.3$, $p_2 = 0.5$ and $p_3 = 0.2$. Scenario 3: All contributions are different: $N_1 = 1000$, $N_2 = 800$, $N_3 = 500$ and $p_1 = 0.3$, $p_2 = 0.5$ and $p_3 = 0.2$. SD stands for standard deviation.

Scenario	d (cM)	c	Empirical $r^2 \pm$ SD ($\times 10^3$)	$Q_{eq,00} \times 10^3$	$L_{eq,00} \times 10^3$
1	5	0.0476	2.916 ± 4.105	2.406	2.905
1	10	0.0906	1.668 ± 2.354	1.166	1.666
1	20	0.1648	1.044 ± 1.474	0.551	1.051
1	50	0.3161	0.705 ± 0.999	0.201	0.701
1	∞	0.5	0.574±0.815	0.071	0.571
2	5	0.0476	3.049 ± 4.256	2.539	3.038
2	10	0.0906	1.741 ± 2.453	1.234	1.733
2	20	0.1648	1.084 ± 1.528	0.586	1.086
2	50	0.3161	0.718 ± 1.013	0.216	0.715
2	∞	0.5	0.583±0.824	0.078	0.578
3	5	0.0476	3.572 ± 5.043	2.940	3.439
3	10	0.0906	1.995 ± 2.813	1.435	1.935
3	20	0.1648	1.224 ± 1.723	0.687	1.187
3	50	0.3161	0.772 ± 1.090	0.257	0.757
3	∞	0.5	0.598±0.846	0.094	0.594

Table 2: Results for estimated N_0 evaluated for three scenarios, for different genetic distances (d) which correspond to different recombination rates (c). Results are given evaluated using r^2 obtained via for L_{00}, using 100 and 500 pair of loci. Scenario 1: All contributions are the same (i.e. all N_i's take the same value equal to 1000 individuals) and $p_1 = p_2 = p_3 = \frac{1}{3}$. Scenario 2: All contributions are the same (all $N_i = 1000$ individuals), but $p_1 = 0.3$, $p_2 = 0.5$ and $p_3 = 0.2$. Scenario 3: All contributions are different: $N_1 = 1000$, $N_2 = 800$, $N_3 = 500$ and $p_1 = 0.3$, $p_2 = 0.5$ and $p_3 = 0.2$.

Scenario	d	c	Empirical $r^2 \times 10^3$	Mean	SD_{100}	SD_{500}
1	5	0.0476	2.875	991.24	145.19	65.24
1	10	0.0906	1.657	996.31	143.85	63.40
1	20	0.1648	1.051	1005.66	145.45	63.97
1	50	0.3161	0.701	994.24	144.67	63.01
1	∞	0.5	0.574	996.16	140.77	65.58
2	5	0.0476	3.049	996.67	145.50	62.01
2	10	0.0906	1.733	993.18	139.80	58.52
2	20	0.1648	1.087	999.98	145.68	63.53
2	50	0.3161	0.713	995.94	152.03	63.74
2	∞	0.5	0.583	991.48	140.64	60.48
3	5	0.0476	3.540	956.48	141.35	60.35
3	10	0.0906	1.994	966.77	143.50	64.65
3	20	0.1648	1.227	968.07	138.63	60.84
3	50	0.3161	0.772	980.36	141.15	62.30
3	∞	0.5	0.598	992.85	138.76	62.15

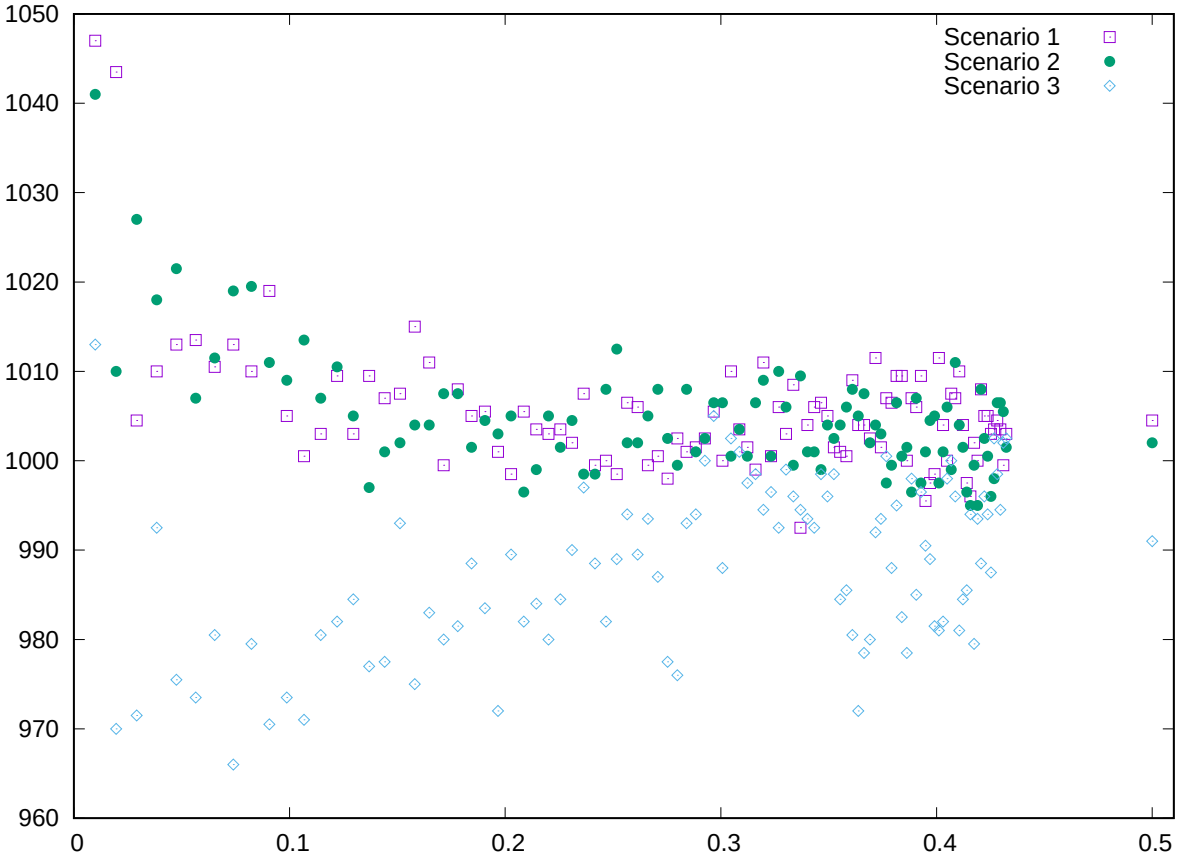

Figure 4: Inferred N_0 for a population with true $N_0 = 1000$ individuals, under three different scenarios. Values are averages over 100000 replicates.

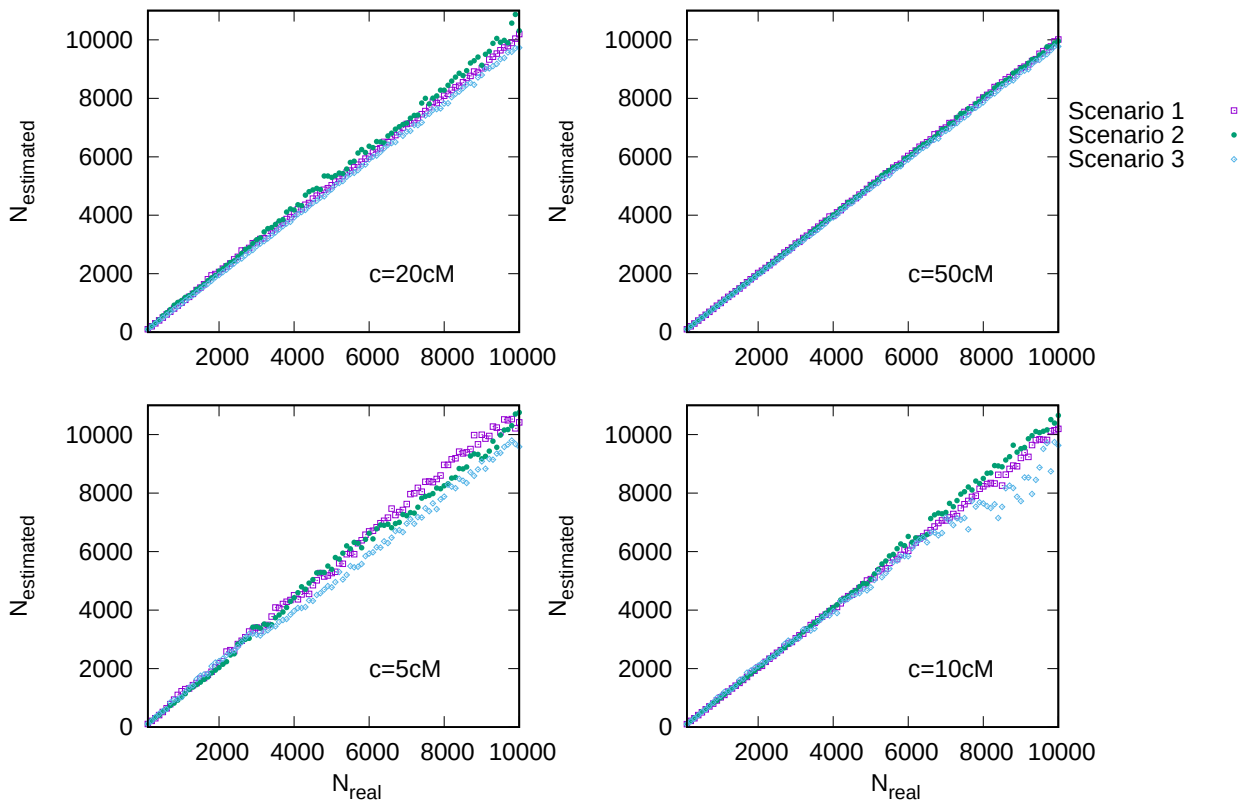

Figure 5: Inferred N_0 for a population with varying N_0 individuals, under three different scenarios. Recombination distances are fixed at 5cM, 10 cM, 20 cM and 50 cM, from bottom to top. Values are averages over 100000 replicates.

Scenario	Markers	Chromosomes	N_0	SD
1	1000	1	999.86	15.88
1	5000	1	999.69	14.44
1	1000	5	999.70	5.34
1	5000	5	999.34	4.25
1	1000	10	999.46	4.25
1	5000	10	999.43	3.32
2	1000	1	998. 77	15.99
2	5000	1	998.77	15.24
2	1000	5	999.38	5.63
2	5000	5	999.35	4.49
2	1000	10	999.69	4.83
2	5000	10	999.37	3.47
3	1000	1	999.46	17.48
3	5000	1	998.93	16.36
3	1000	5	998.98	6.12
3	5000	5	1000.00	4.91
3	1000	10	999.42	4.98
3	5000	10	999.76	3.90

Table 3: Mean N_0 for each scenario using simulations of 1000 or 5000 markers in 1, 5 or 10 chromosomes. Standard deviation was calculated over 1000 replicates. Scenario 1: All contributions are the same (i.e. all N_i's take the same value equal to 1000 individuals) and $p_1 = p_2 = p_3 = \frac{1}{3}$. Scenario 2: All contributions are the same (all $N_i = 1000$ individuals), but $p_1 = 0.3$, $p_2 = 0.5$ and $p_3 = 0.2$. Scenario 3: All contributions are different: $N_1 = 1000$, $N_2 = 800$, $N_3 = 500$ and $p_1 = 0.3$, $p_2 = 0.5$ and $p_3 = 0.2$.

Individuals used	S	Corrected R^2	N_0	N_e	`Ne estimator`
Nuttalli	33	0.000766	1418.88 ± 94.73	525.06 ± 35.07	433.4 ± 28.96
Pugetensis	71.1	0.000264	4117.43 ± 116.63	1524.01 ± 43.17	1260.6 ± 35.57

Table 4: Estimated N_0 and N_e for white-crowned sparrow, together with `Ne estimator` results (Waples & Do 2008). S is the weighted harmonic mean of the sample size. R^2 is a measure of linkage disequilibrium from unphased data, corrected by sample size.

461

Subspecies	N_e		`Ne estimator`	
	$p = 0$	$p = 0.05$	$p = 0$	$p = 0.05$
Nuttalli	525.06 ± 35.07	239.33± 7.32	433.4 ± 28.96	196.40 ± 6.05
Pugetensis	1524.01 ± 43.17	745.27 ± 17.70	1260.6 ± 35.57	615.51 ± 14.62

Table 5: Dependence on minor allele frequency (MAF) of the estimates of N_0 and N_e. A MAF $p = 0$ means no locus has been filtered, while at $p = 0.05$ those loci with alleles with minor allele frequency lower or equal to 0.05 have been removed from the analysis.